



OPEN ACCESS

EDITED BY

Luiz A. Manzoni,
Concordia College, United States

REVIEWED BY

Andrzej Wereszczyński,
Jagiellonian University, Poland
João Guilherme Ferreira Campos,
Universidade de Pernambuco, Brazil

*CORRESPONDENCE

J. Mateos Guilarte,
✉ guilarte@usal.es

RECEIVED 16 June 2025

REVISED 23 July 2025

ACCEPTED 02 December 2025

PUBLISHED 17 February 2026

CITATION

Guilarte JM (2026) Low-energy dynamics of vibrating kinks.
Front. Phys. 13:1647949.
doi: 10.3389/fphy.2025.1647949

COPYRIGHT

© 2026 Guilarte. This is an open-access article distributed under the terms of the [Creative Commons Attribution License \(CC BY\)](https://creativecommons.org/licenses/by/4.0/). The use, distribution or reproduction in other forums is permitted, provided the original author(s) and the copyright owner(s) are credited and that the original publication in this journal is cited, in accordance with accepted academic practice. No use, distribution or reproduction is permitted which does not comply with these terms.

Low-energy dynamics of vibrating kinks

J. Mateos Guilarte*

Instituto Universitario de Física Fundamental y Matemáticas, Universidad de Salamanca, Salamanca, Spain

The low-energy dynamics of kinks and kink–antikink configurations in the Jackiw–Rebbi model are fully described. The strategy is based on the collective coordinates adiabatic approach. The necessary solution of quantum mechanical spectral problems, for both scalar and spinorial wave functions, is revealed as an intermediate step.

KEYWORDS

kink adiabatic dynamics, fermionic kink fluctuations, kink–Dirac operators, energy transfer between kinetic and potential forms, bosonic versus fermionic effective potential wells in KAK configurations

1 Introduction

Throughout the last 50 years, a vast research activity studying the dynamics of topological defects has experienced a strong impetus. Given the relevance of topological defects in fundamental/mathematical physics, condensed matter physics, cosmology, biophysics, and other branches of science, this task revealed itself as necessary. Except in integrable field theories like sine-Gordon, Korteweg–de Vries, and Kadomtsev–Petviashvili equations, no analytical methods are applicable. Recently, however, numerical methods have been successfully applied to analyze scattering of kinks in several distinguished non-integrable modes that live in $(1+1)$ -dimensions. We mention specifically [1–3], where numerical methods of integration have been applied to understand processes of scattering between kinks and antikinks. Focusing on analyzing collisions between kink-shaped defects, either simply traveling and/or wobbling while traveling, success in understanding their interactions emerged. Of course, a vast literature on this subject can be found in the references just quoted. A parallel attack to the understanding of interaction between topological defects has been alternatively produced from the adiabatic, low-energy side. Time dependence is restricted to the so-called collective coordinates, and the investigation deals with dynamical systems with a finite number of degrees of freedom. Specifically, when the objects of research are kinks, the central topic in this article, the solution of the simplified system in [4] shows astonishing qualitative agreement with the numerical results.

In one *a priori* completely different framework, much research has been devoted to studying how fermions affect the dynamics of systems in field theory and condensed matter physics; see [5–7]. A new phenomenon with far-reaching consequences was discovered in these articles: the fractionization of the Fermi number in the presence of topological defects; see also [8], where the connection with index theorems, specifically the eta invariant, was explored. These findings aroused interest in studying physical settings where fermions live in the presence of topological defects, such as kinks; see, for example, [9, 10, 14].

In this work, we shall concentrate on developing the collective coordinates adiabatic approximation when fermions are present in the system. A previous work in this line is [13], but our focus will be the paradigmatic Jackiw–Rebbi model, a simple setting rich enough to obtain a great amount of information. More precisely, we shall continue the analysis developed in [11, 12] to fully unveil the adiabatic dynamics of vibrating kinks and kink–antikink configurations.

2 The Jackiw–Rebbi model in $\mathbb{R}^{1,1}$ Minkowski space-time

Let us consider a quantum field theory (QFT) of fermions and bosons restricted to move on a line. The dynamics is governed by the action:

$$S_{JR}[\phi, \Psi] = \int_{\mathbb{R}^{1,1}} d^2x \left\{ \frac{1}{2} \partial_\mu \phi \partial^\mu \phi - \frac{\lambda^2}{2} (\phi^2 - 1)^2 + i \bar{\Psi} \gamma^\mu \partial_\mu \Psi - g \bar{\Psi} \phi \Psi \right\}$$

$$\bar{\Psi} = \Psi^\dagger \gamma^0, [\phi] = 1, [\Psi] = L^{-1/2}, [\lambda] = L^{-1} = [g], \tag{1}$$

encompassing a quartic self-interaction of the bosons plus a Yukawa coupling between fermions and bosons. In the natural system of units where the Planck constant and the speed of light in vacuum are set to one, $\hbar = c = 1$, the dimensions of the fields and couplings are shown below the action above. The Jackiw–Rebbi Hamiltonian $H = H_{FB} + H_B$ is, in turn, obtained via a Legendre transformation:

$$H_{FB} = \int dx \Psi^\dagger(t, x) \left\{ -i \alpha \frac{\partial}{\partial x} \right\} \Psi(t, x) + \int dx \Psi^\dagger(t, x) \{ g \phi(t, x) \beta \} \Psi(t, x)$$

$$H_B = \frac{1}{2} \int dx \left\{ \Pi^2(x) + \left(\frac{\partial \phi}{\partial x} \right)^2 + \lambda^2 (\phi^2(t, x) - 1)^2 \right\}. \tag{2}$$

The Dirac matrices $\alpha = \sigma_2$ and $\beta = \sigma_1$ are chosen like in [5]. Here, σ_1 and σ_2 are Pauli matrices, and this choice corresponds to the Clifford algebra

$$\gamma^0 = \sigma_1, \gamma^1 = i \sigma_3, \gamma^5 = \gamma^0 \gamma^1 = \sigma_2$$

$$[\gamma^\mu, \gamma^\nu] = 2 g^{\mu\nu}, \quad g^{\mu\nu} = \text{diag}(1, -1), \quad \mu, \nu = 0, 1.$$

The Klein–Gordon and Dirac fields are maps from the Minkowski space, respectively, to the field of the reals and the fundamental irreducible representation of the **Spin**(1, 1; \mathbb{R}) group:

$$\phi(t, x) \in \mathbb{R}^{1,1} \rightarrow \mathbb{R}, \quad \Psi(t, x) = \begin{pmatrix} \psi_1(t, x) \\ \psi_2(t, x) \end{pmatrix}: \mathbb{R}^{1,1} \rightarrow \text{irr}_p \mathbf{Spin}(1, 1; \mathbb{R}),$$

that is, the transformations generated by $[\gamma^0, \gamma^1]$, and characterized by the Lorentz boost parameter χ , acts on one spinor in the form

$$S_L[\chi] = e^{\frac{\chi}{4} [\gamma^0, \gamma^1]} = \begin{pmatrix} \cosh \frac{\chi}{2} & i \sinh \frac{\chi}{2} \\ -i \sinh \frac{\chi}{2} & \cosh \frac{\chi}{2} \end{pmatrix},$$

$$\cosh \chi = \frac{1}{\sqrt{1 - v^2}}, \quad \Psi_L(t, x) = S_L[\chi] \Psi(t, x).$$

The Euler–Lagrange (classical) field equations read

$$\phi + 2\lambda^2 \phi(t, x) (\phi^2(t, x) - 1) + g \bar{\Psi}(t, x) \Psi(t, x) = 0, \tag{3}$$

$$i \gamma^\mu \frac{\partial \Psi}{\partial x^\mu} - g \phi(t, x) \Psi(t, x) = 0. \tag{4}$$

This system of coupled non-linear partial differential equations (PDEs) is very difficult to solve. The situation is better and pertinent to the posterior canonical quantization of the system if some static solution of the system of the form $(\phi_S(x), \Psi_S = 0)$ is discovered:

$$-\frac{d^2 \phi_S}{dx^2} + 2\lambda^2 \phi_S(x) (\phi_S^2(x) - 1) = 0.$$

In that case, one may search for solutions close to these static solutions that linearize the (3-4) PDE system:

$$\phi(t, x) = \phi_S(x) + \eta(t, x) \Rightarrow \eta + 2\lambda^2 (3\phi_S^2(x) - 1) \eta(t, x) = \mathcal{O}(\eta^2), \tag{5}$$

$$i \gamma^\mu \frac{\partial \Psi}{\partial x^\mu} - g \phi_S(x) \Psi(t, x) = \mathcal{O}(\eta \Psi). \tag{6}$$

Because the terms in Equations 5 and 6 with no derivatives of the fields are time independent, it is convenient to solve the linear system via a Fourier transform in time:

$$\eta(t, x) = \int_{-\infty}^{\infty} \frac{d\omega_B}{2\pi} e^{i\omega_B t} \eta(x; \omega_B), \quad \Psi(t, x) = \int_{-\infty}^{\infty} \frac{d\omega_F}{2\pi} e^{i\omega_F t} \Psi(x; \omega_F).$$

The linear PDE system (Equations 5 and 6) becomes equivalent to the spectral problem:

$$h_{\text{Sch}} \eta(x; \omega_B) = \left[-\frac{d^2}{dx^2} + 2\lambda^2 (3\phi_S^2(x) - 1) \right] \eta(x; \omega_B) = \omega_B^2 \eta(x; \omega_B), \tag{7}$$

$$h_{\text{D}} \Psi(x; \omega_F) = \left[-i\alpha \frac{d}{dx} + g\beta\phi_S(x) \right] \Psi(x; \omega_F) = \omega_F \Psi(x; \omega_F), \tag{8}$$

where h_{Sch} and h_{D} are, respectively, the quantum mechanical Schrödinger and Dirac operators in the background created by the ϕ_s classical solution.

2.1 Bose–Fermi quanta in homogeneous field backgrounds

The standard canonical quantization procedure to build the space of stationary states of H and evaluate the quantum transitions within the Fock space states is based on finding the eigenwave functions of the Schrödinger operator and the eigenspinors of the Dirac operator to be taken as the one-particle states. The simplest solutions of the classical field equations are the two homogeneous, independent of t and x , minima of the scalar potential energy, whereas H_{BF} is minimized by $\Psi_V = 0$:

$$\phi_S(t, x)^\pm = \phi_V^\pm = \pm 1, \quad \Psi_S(x) = \Psi_V = 0.$$

Choosing one of these two configurations, for example, $(\phi_S(t, x)^+ = +1, \Psi_S(t, x) = 0)$, as the ground state, spontaneously breaks the $\phi \rightarrow -\phi$ symmetry, and the linear Klein–Gordon and Dirac equations become:

$$\frac{\partial^2 \phi}{\partial t^2} = \frac{\partial^2 \phi}{\partial x^2} - 4\lambda^2 \phi(t, x), \tag{9}$$

$$\begin{pmatrix} i\frac{\partial}{\partial t} & 0 \\ 0 & i\frac{\partial}{\partial t} \end{pmatrix} \cdot \begin{pmatrix} \psi_1(t, x) \\ \psi_2(t, x) \end{pmatrix} = \begin{pmatrix} 0 & -\frac{\partial}{\partial x} + g \\ \frac{\partial}{\partial x} + g & 0 \end{pmatrix} \cdot \begin{pmatrix} \psi_1(t, x) \\ \psi_2(t, x) \end{pmatrix}. \tag{10}$$

Because there are no time- and space-dependent terms in the PDE operators in the linear Equations 9 and 10, it is convenient to search for the general solutions as Fourier transform integrals¹

$$\phi(t, x) = \int_{\mathbb{H}^+} \frac{dk}{\sqrt{4\pi\omega_B(k)}} \left[a(k) e^{-i\omega_B(k)t + ikx} + a^*(k) e^{i\omega_B(k)t - ikx} \right], \tag{11}$$

$$\Psi(t, x) = \sqrt{g} \int_{\mathbb{H}^+} \frac{dk}{\sqrt{4\pi\omega_F(k)}} \left[b(k) u(k) e^{-i\omega_F(k)t + ikx} + c^*(k) v(k) e^{i\omega_F(k)t - ikx} \right], \tag{12}$$

$$\Psi^\dagger(t, x) = \sqrt{g} \int_{\mathbb{H}^+} \frac{dk}{\sqrt{4\pi\omega_F(k)}} \left[b^*(k) u^\dagger(k) e^{i\omega_F(k)t - ikx} + c(k) v^\dagger(k) e^{-i\omega_F(k)t + ikx} \right], \tag{13}$$

where the integration is performed over the upper branches \mathbb{H}_B^+ and \mathbb{H}_F^+ of the hyperbolas: $\omega_B^2 = k^2 + 4\lambda^2$, $\omega_B = +\sqrt{k^2 + 4\lambda^2}$, and $\omega_F^2 = k^2 + g^2$, $\omega_F = +\sqrt{g^2 + k^2}$.

¹ We denote back $\eta(t, x)$ as $\phi(t, x)$ to follow the conventional notation.

In order to be the spinor expansion (Equation 12), the general solution of Equation 10, $u(k)$ and $v(k)$ must be, respectively, the eigenspinors of the 2×2 -matrices with eigenvalues ω_F^2 :

$$\begin{aligned} \begin{pmatrix} 0 & g-ik \\ g+ik & 0 \end{pmatrix} \cdot \begin{pmatrix} u_1(k) \\ u_2(k) \end{pmatrix} &= +\sqrt{k^2+g^2} \begin{pmatrix} u_1(k) \\ u_2(k) \end{pmatrix}, \\ \begin{pmatrix} 0 & -g-ik \\ -g+ik & 0 \end{pmatrix} \cdot \begin{pmatrix} v_1(k) \\ v_2(k) \end{pmatrix} &= +\sqrt{k^2+g^2} \begin{pmatrix} v_1(k) \\ v_2(k) \end{pmatrix}, \\ u(k) &= +\left(\frac{\sqrt{k^2+g^2}}{2g}\right)^{1/2} \cdot \begin{pmatrix} 1 \\ \frac{g+ik}{\sqrt{k^2+g^2}} \end{pmatrix}, \\ v(k) &= \left(\frac{\sqrt{k^2+g^2}}{2g}\right)^{1/2} \cdot \begin{pmatrix} \frac{-g-ik}{\sqrt{k^2+g^2}} \\ 1 \end{pmatrix}, \end{aligned}$$

which satisfy the standard orthonormality conditions:

$$u^\dagger(k)u(k) = \frac{\omega_F}{g} = v^\dagger(k)v(k), \quad \bar{u}(k)u(k) = 1 = -\bar{v}(k)v(k),$$

together with $u^\dagger(k)v(-k) = 0$.

In the canonical quantization procedure, the Fourier coefficients of the scalar field are promoted to creation and annihilation bosonic operators satisfying the commutation rules:

$$[\hat{a}(k_1), \hat{a}^\dagger(k_2)] = \delta(k_1 - k_2), \quad [\hat{a}(k_1), \hat{a}(k_2)] = 0 = [\hat{a}^\dagger(k_1), \hat{a}^\dagger(k_2)].$$

The ground state with no meson particles at all is annihilated by all the destruction bosonic operators

$$\hat{a}(k)|0\rangle_B = 0, \quad \forall k.$$

Meson multiparticle states have the form

$$\prod_{j=1}^N [\hat{a}^\dagger(k_j)]^{n_j} |0\rangle_B = |n_1 n_2 \dots n_N\rangle, \quad n_j \in \mathbb{N}, \quad \sum_{j=1}^N n_j = N, \tag{14}$$

and form the basis of the bosonic Fock space, obtained via the symmetric tensor product.

Simile modo, the canonical quantization of the Dirac field courses via anticommutation relationships

$$\{\hat{b}^\dagger(k_1), \hat{b}(k_2)\} = \delta(k_1 - k_2), \quad \{\hat{c}^\dagger(k_1), \hat{c}(k_2)\} = \delta(k_1 - k_2), \tag{15}$$

$$\{\hat{b}(k_1), \hat{b}(k_2)\} = 0 = \{\hat{c}(k_1), \hat{c}(k_2)\}. \tag{16}$$

Likewise, the ground state with neither electrons nor positrons is annihilated by all the fermionic destruction operators.

$$\hat{b}(k)|0\rangle_F = \hat{c}(k)|0\rangle_F, \quad \forall k. \tag{17}$$

Electron/positron³ multiparticle states form the basis of the fermionic Fock space built from the one-particle states via antisymmetric tensor product:

$$\prod_{j=1}^N [\hat{b}^\dagger(k_j)]^{n_j^-} |0\rangle_F = |n_1^- n_2^- \dots n_N^-\rangle, \quad n_j^- = 0 \text{ or } 1, \quad \sum_{j=1}^N n_j^- = N, \tag{18}$$

$$\prod_{j=1}^N [\hat{c}^\dagger(k_j)]^{n_j^+} |0\rangle_F = |n_1^+ n_2^+ \dots n_N^+\rangle, \quad n_j^+ = 0 \text{ or } 1, \quad \sum_{j=1}^N n_j^+ = N. \tag{19}$$

Quantization by anticommutators forces the antisymmetry of the multiparticle states, and thus one state can only be either unoccupied, $n_j^\pm = 0$, or occupied only by one Fermion, $n_j^\pm = 1$. Note that $n_j^+ = 1$ and $n_j^- = 1$ are simultaneously possible describing one state with one electron and one positron, both with momentum k_j .

2 Note, however, that the spectral equation for u is the same as the spectral equation for v if (ω_F, k) is replaced by $(-\omega_F, -k)$. Notice also that it is possible to come back to (ω_F, k) , provided that g will be transmuted to $-g$, the essential property of antimatter.

3 We shall refer to the Fermi quanta in the Jackiw–Rebbi model as electrons/positrons by analogy with quantum electrodynamics (QED). In the JR system, there is no electric charge. The Nöther’s invariant associated to the $U(1)$ symmetry is the Fermi number.

3 Bosonic and fermionic kink fluctuations

In addition to the homogeneous static solutions, this system also admits static space-dependent solutions that are traveling waves with kink shape via Lorentz transformations:

$$\begin{aligned}
 -\frac{d^2\phi}{dx^2} \pm 2\lambda^2\phi(x)(\phi^2 - 1) = 0 &\Leftrightarrow \phi_K^\pm\left(\frac{x-vt}{\sqrt{1-v^2}} - a\right) = \pm \tanh\left[\lambda\left(\frac{x-vt}{\sqrt{1-v^2}} - a\right)\right] \\
 -i\alpha\frac{d\Psi_K}{dx} + \beta(g\phi_K + im\alpha)\Psi_K = 0 &\Leftrightarrow \Psi_K = 0.
 \end{aligned}$$

Defining non-dimensional space-time coordinates $\tau = \lambda t, y = \lambda x$ and considering small fluctuations,

$$\phi(\tau, y) \simeq \phi_K(y) + \eta(\tau, y), \quad \Psi(\tau, y) = 0 + \psi(\tau, y).$$

In the kink's classical background, the expansion above is still a solution of the field equations if the linear system of coupled PDEs holds:

$$\begin{aligned}
 \left(\frac{\partial^2}{\partial\tau^2} - \frac{\partial^2}{\partial y^2} + 4 - \frac{6}{\cosh^2 y}\right)\phi(\tau, y) &= \mathcal{O}(\phi^2), \\
 \left(i\frac{\partial}{\partial\tau} - i\sigma_2\frac{\partial}{\partial y} + v\sigma_1\phi_K(y)\right)\Psi(\tau, y) &= \mathcal{O}(\phi\Psi).
 \end{aligned}$$

Note that (1) we choose $\Psi_K = 0$ as the fermionic ground state, and thus, we neglected the fermionic backreaction on the kink at the classical level. (2) We introduce the important non-dimensional parameter $v = \frac{g}{\lambda}$ that measures the strength of the Yukawa versus the scalar self-interaction couplings. (3) Again, we abuse notation in the linearized equations by writing $\phi(\tau, y)$ instead of $\eta(\tau, y)$. Because there are no τ -dependent terms in both operators, it is natural that the search for solutions via τ -Fourier transform integrals:

$$\begin{aligned}
 \phi(\tau, y) &= \int_{-\infty}^{\infty} d\tau e^{i\Omega_B\tau} f_{\Omega_B}(y), \quad \Omega_B = \frac{\omega_B}{\lambda}, \\
 \Psi(\tau, y) &= \int_{-\infty}^{\infty} d\tau e^{i\Omega_F\tau} \psi_{\Omega_F}(y), \quad \Omega_F = \frac{\omega_F}{\lambda},
 \end{aligned}$$

such that the general solution of the linearized equations requires the solution of two quantum mechanical spectral problems, one for a Pösch-Teller/Schrödinger operator, and the other one for a Dirac operator in a kink potential background.

3.1 Higgs bosons propagating over kink topological defects

Starting with the scalar/Bose case, the quantum mechanical spectral problem governing the scalar kink fluctuations reads

$$h_{PT}f_B(y) = \left(-\frac{d^2}{dy^2} + 4 - \frac{6}{\cosh^2 y}\right)f_{\Omega_B}(y) = \Omega_B^2 f_{\Omega_B}(y). \tag{20}$$

Fortunately, the eigenvalues and eigenfunctions of this one-particle Hamiltonian are well known. The discrete spectrum possesses two bound state eigenfunctions whose corresponding eigenvalues s are, respectively, $\Omega_B^2 = 0$ and $\Omega_B^2 = 3$, namely:

3.1.1 Zero mode

$$\Omega_0 = 0, \quad f_0(y) = \frac{1}{\cosh^2 y}.$$

This eigenfunction is due to the spontaneous breaking of the translational symmetry by the kink.

3.1.2 Bound state: the shape fluctuation mode

$$\Omega_{\sqrt{3}}^2 = 3, \quad f_{\sqrt{3}}(y) = \frac{\sinh y}{\cosh^2 y}.$$

The next eigenfunction in the discrete spectrum responds to vibrations of the kink, rather than translations, with a frequency of $\sqrt{3}$, and it is referred to as shape mode because it is accompanied by variations in the kink shape.⁴

Above these two bound fluctuation modes, the eigenstates with energies over the threshold of the continuous spectrum $\Omega_B^2(0) = 4$ arise.

4 This fluctuation mode is closely approximated by a Derrick mode obeying a Lorentz dilatation; see [4].

3.1.3 Scattering states: the continuous spectrum

$$\Omega_B^2(q) = q^2 + 4, \quad f(y; q) = e^{iqy} (3 \tanh^2 y - 3iq \tanh y - (1 + q^2)) = e^{iqy} P_2(\tanh y; q).$$

Remarkably, the scattering involved is transparent; that is, the reflection amplitude $r(q)$ is zero, and the modulus of the transmission amplitude is one

$$t(q) = \frac{1 - iq}{1 + iq} \cdot \frac{2 - iq}{2 + iq}.$$

From it, the total phase shift and the spectral density are easily computed. The general solution is obtained as a linear superposition in terms of the eigenfunctions of the one-particle operator

$$\begin{aligned} \phi(\tau, y) = & \lim_{\varepsilon \rightarrow 0} (A_0 e^{-i\varepsilon\tau} + A_0^* e^{i\varepsilon\tau}) f_0(y) + (A_{\sqrt{3}} e^{-i\sqrt{3}\tau} + A_{\sqrt{3}}^* e^{i\sqrt{3}\tau}) \cdot f_{\sqrt{3}}(y) \\ & + \int \frac{dq}{\sqrt{2\sqrt{q^2 + 4}}} \left(A(q) e^{-i\sqrt{q^2 + 4}\tau} f(y; q) + A^*(q) e^{i\sqrt{q^2 + 4}\tau} f^*(y; q) \right). \end{aligned} \tag{21}$$

Canonical quantization courses, as usual, replace the complex coefficients of the spectral expansion by quantum operators satisfying commutative quantization relationships:

$$[\widehat{A}_0, \widehat{A}_0^\dagger] = 1, \quad [\widehat{A}_{\sqrt{3}}, \widehat{A}_{\sqrt{3}}^\dagger] = 1, \quad [\widehat{A}(q_1), \widehat{A}^\dagger(q_2)] = \delta(q_1 - q_2).$$

The differences with respect to the bosonic Fock space in the vacuum sector are three: (1) there is one state where a boson is bounded to the kink center, traveling with it at no cost of energy. (2) The shape mode is one state in the Fock space where one boson is trapped by the kink, giving rise to one kink excited state characterized by its vibration frequency. (3) There are many states where the Higgs quanta are scattered off the kink, but the outgoing particle waves escape from the kink center as plane waves times Jacobi polynomials of order 2.

3.2 Electrons/positrons propagating over kink topological defects

Spinorial kink fluctuations are determined from the spectral problem of the one-particle kink–Dirac Hamiltonian:

$$\begin{aligned} h_{DK} \psi(y; \Omega_F) = \Omega_F \psi(y; \Omega_F), \quad \psi(y; \Omega_F) = \frac{1}{\sqrt{g}} \begin{pmatrix} \psi_1(y; \Omega_F) \\ \psi_2(y; \Omega_F) \end{pmatrix}, \\ h_{DK} = \begin{pmatrix} 0 & -\frac{d}{dy} + v \tanh y \\ \frac{d}{dy} + v \tanh y & 0 \end{pmatrix}, \quad v = \frac{g}{\lambda}, \quad [\psi_1(y; \Omega_F)] = [\psi_2(y; \Omega_F)] = 1. \end{aligned} \tag{22}$$

Instead of directly solving the spectral problem (Equation 22), we notice that the square of the Dirac–kink operator is a diagonal matrix of contiguous Pösch–Teller–Schrödinger operators. Moreover, defining the first-order differential operator $d_v = \frac{d}{dy} + v \tanh y$, the Darboux factorization method may be successfully applied to find the spectrum.

$$\begin{aligned} h_{DK}^2 = & \begin{pmatrix} -\frac{d^2}{dy^2} + v^2 - \frac{v(v+1)}{\cosh^2 y} & 0 \\ 0 & -\frac{d^2}{dy^2} + v^2 - \frac{v(v-1)}{\cosh^2 y} \end{pmatrix} \\ = & \begin{pmatrix} d_v^\dagger d_v & 0 \\ 0 & d_v d_v^\dagger \end{pmatrix} = \begin{pmatrix} d_v^\dagger d_v & 0 \\ 0 & d_{v-1}^\dagger d_{v-1} + 2v - 1 \end{pmatrix}. \end{aligned}$$

3.2.1 Fermionic zero modes

One immediately recognizes fermionic zero modes and the non-existent normalizable anti-fermionic zero modes as living, respectively, in the kernels of d_v or d_v^\dagger . One finds

$$h_{DK} \begin{pmatrix} \psi_1^{(0)}(y) \\ 0 \end{pmatrix} = 0 \Rightarrow \psi_1^{(0)}(y) = \frac{1}{\cosh^v y}, \quad h_{DK} \begin{pmatrix} 0 \\ \psi_2^{(0)}(y) \end{pmatrix} = 0 \Rightarrow \psi_2^{(0)}(y) = \cosh^v y.$$

Needless to say, changing from kink to antikink, the normalizable zero mode corresponds to antifermions.

3.2.2 Fermionic kink shape modes

Focusing on the case when g is a multiple of λ , and $\nu = N \in \mathbb{N}^*$ is a positive natural number, there are $N - 1$ proper bound states that correspond to vibrating kink spinorial shape modes. The eigenvalues are well known and show that these states carry imaginary momentum on the positive imaginary half-axis in the complex q -plane: $q = i\kappa_l^5$.

Eigenvalues:

$$\Omega_F^{(l)}(\kappa_l; N) = \sqrt{(2N - l)l} = \sqrt{N^2 - \kappa_l^2}, \quad l = 1, 2, \dots, N - 1, \quad \kappa_l = N - l.$$

For the truncated-to-polynomial hypergeometric Gauss series, the eigenspinors are also explicitly known.

Eigenspinors $\psi^{(l)}(y) = \begin{pmatrix} \psi_1^{(l)}(y) \\ \psi_2^{(l)}(y) \end{pmatrix}$

$$\begin{aligned} \psi_1^{(l)}(y) &= \frac{1}{\cosh^{N-l} y} \cdot {}_2F_1\left(2N + 1 - l, -l, N - l + 1; \frac{1}{2}(1 + \tanh y)\right), \\ \psi_2^{(l)}(y) &= \frac{1}{\cosh^{N-l} y} \cdot {}_2F_1\left(2N - l, -l + 1, N - l + 1; \frac{1}{2}(1 + \tanh y)\right). \end{aligned}$$

This identification has been possible because the bound state labeled by l in the upper diagonal component and the bound state labeled by $j = l - 1$ in the lower diagonal component of the square of the Dirac operator share identical eigenvalues.

3.2.3 Fermions scattered off kinks

It remains to describe the spinorial fluctuations scattered off kinks, that is, not bounded to the kink center. Of course, these fluctuations belong to the continuous spectrum of h_{DK} :

$$h_{DK}\psi(y; q) = \Omega_F(q) \psi(y, q), \quad \psi(y; q) = \begin{pmatrix} \psi_1(y; q) \\ \psi_2(y; q) \end{pmatrix}. \tag{23}$$

The eigenvalues are

Eigenvalues: $\Omega_F^2(q) = q^2 + N^2 \Rightarrow \Omega_F(q) = +\sqrt{q^2 + N^2}$

Whereas the eigenspinors are proper Gauss hypergeometric series:

Eigenspinors

$$\begin{aligned} \psi_1(y; q) &= A(q) (\operatorname{sech} y)^{-iq} \cdot {}_2F_1\left[1 - iq + N, -iq - N, 1 - iq; \frac{e^y}{e^y + e^{-y}}\right], \\ \psi_2(y; q) &= A(q) (\operatorname{sech} y)^{-iq} \cdot {}_2F_1\left[-iq + N, -iq - N + 1, 1 - iq; \frac{e^y}{e^y + e^{-y}}\right]. \end{aligned}$$

Scattering scalar or spinor waves are characterized by their phase shifts and/or spectral densities. Considering the system defined on a finite interval of very large length L with periodic boundary conditions (PBC), the spectral densities of the scattering through the kink wells suffered, respectively, by the upper and lower components are

$$\begin{aligned} \rho_F(q) &= \rho_F^{(1)}(q) + \rho_F^{(2)}(q), \\ \rho_F^{(1)} &= \frac{gL}{2\pi} + \sum_{j=1}^{N-1} \frac{j}{j^2 + q^2} + \frac{N}{N^2 + q^2}, \quad \rho_F^{(2)} = \frac{gL}{2\pi} + \sum_{j=1}^{N-1} \frac{j}{j^2 + q^2}. \end{aligned}$$

Note that, in addition to the precise characterization of the continuous spectrum in terms of the wave number q , the bound states resurface as poles in the spectral density.

3.3 Fermionic quanta

To finish this section, we first expand the classical spinor field in terms of the one-particle states:

$$\begin{aligned} \frac{1}{\sqrt{g}} \Psi^+(y) &= B_0 \begin{pmatrix} \operatorname{sech}^N y \\ 0 \end{pmatrix} + \sum_{l=1}^{N-1} \left[B_l \begin{pmatrix} \psi_1^{(l)}(y) \\ \psi_2^{(l)}(y) \end{pmatrix} e^{-i\Omega_F^{(l)}gt} + C_l^* \begin{pmatrix} \phi_1^{*(l)}(y) \\ \phi_2^{*(l)}(y) \end{pmatrix} e^{i\Omega_F^{(l)}gt} \right] \\ &+ \int \frac{dq}{\sqrt{4\pi\Omega_F(q)}} \left[B(q) \begin{pmatrix} \psi_1(y; q) \\ \psi_2(y; q) \end{pmatrix} e^{-i\Omega_F(q)gt} + C^*(q) \begin{pmatrix} \phi_1^*(y; q) \\ \phi_2^*(y; q) \end{pmatrix} e^{i\Omega_F(q)gt} \right]. \end{aligned}$$

5 In this case, there is one half-bound state just at the threshold of the continuous spectrum with $l = N$. These "half-states" do not exist if $\nu \notin \mathbb{N}^*$.

We stress that the eigenspinors ψ of the Dirac–kink operator and of its g to $-g$ transformed ϕ have been taken as a complete system in the space of spinor fields.

The next step is the promotion of the coefficients to Fermi operators, demanding anticommutation rules between them to establish the canonical quantization procedure:

$$\begin{aligned} \{\widehat{B}_0, \widehat{B}_0^\dagger\} &= 1, & \{\widehat{B}_l, \widehat{B}_l^\dagger\} &= \delta_{l_1 l_2}, & \{\widehat{C}_l, \widehat{C}_l^\dagger\} &= \delta_{l_1 l_2}, \\ \{\widehat{B}(q_1), \widehat{B}^\dagger(q_2)\} &= \delta(q_1 - q_2) = \{\widehat{C}(q_1), \widehat{C}^\dagger(q_2)\}, & \{\widehat{\Psi}^+(y_1), i\widehat{\Psi}^{+\dagger}(y_2)\} &= i\delta(y_1 - y_2). \end{aligned}$$

The Fermi ground state and, in general, the fermionic Fock space describing electron/positron multiparticle states with Fermi statistics built in it follow.

As a practical computation, we show the normal ordered Fermi number operator, all the annihilation operators placed at the right of the creation operators denoted by the $:\widehat{F}$: symbol.

$$\begin{aligned} :\widehat{F}: &= \int dx \frac{1}{2} [\widehat{\Psi}^{+\dagger}(x), \widehat{\Psi}^+(x)], & \sigma_1 \begin{pmatrix} \psi_1(y; q) \\ \psi_2(y; q) \end{pmatrix} &= \begin{pmatrix} \phi_1(y; q) \\ \phi_2(y; q) \end{pmatrix} \\ :\widehat{F}: &= \frac{1}{2} [\widehat{B}_0^\dagger, \widehat{B}_0] + \sum_{l=1}^{N-1} (\widehat{B}_l^\dagger \widehat{B}_l - \widehat{C}_l^\dagger \widehat{C}_l) + \int dq \rho_F(q) (\widehat{B}^\dagger(q) \widehat{B}(q) - \widehat{C}^\dagger(q) \widehat{C}(q)) \\ &= \widehat{N}_0 - \frac{1}{2} + \sum_{l=1}^{N_1} (\widehat{N}_l^- - \widehat{N}_l^+) + \int dq \rho_F(q) (\widehat{N}^-(q) - \widehat{N}^+(q)). \end{aligned}$$

Due to the unpaired zero mode, we see that the expectation value of this operator in any state of the fermionic Fock space is fractional. Note that because the σ_1 matrix maps the eigenspinors of $h_{DK}(g)$ into those of $h_{DK}(-g)$, not only are the states in the discrete spectra paired (except the zero mode), but also the spectral densities in the continuous spectra are identical.

4 Low-energy dynamics of vibrating kinks and the impact of bosonic and fermionic shape modes

The study of the dynamics of topological defects in non-linear non-integrable field theories is an endeavor beyond the reach of analytical methods. Numerical analysis on increasingly powerful computers has been successfully used to obtain insights into this important subject because many types of topological defects exist in Nature. During the last 20 years of the twentieth century, an alternative route has been investigated by physicists and mathematicians. The idea is that at low energies, the dynamics is essentially described by geodesic motion over the moduli space of these extended objects. More recently, internal/shape vibrational modes of fluctuation are included in these effective finite-dimensional dynamical systems. The degrees of freedom correspond to the collective coordinates of the defect and its vibrational modes. The adiabatic principle dictates that both the kink moduli space coordinates and the shape mode amplitudes of kink fluctuations support all the time dependence and describe the adiabatic evolution of the topological defect. The miracle is that sticking to this approximation by numerical methods has been confirmed in this simplified scenario.

In this section, our goal is to construct the effective adiabatic dynamics of the kink collective coordinates encompassing both bosonic and fermionic shape fluctuation modes. We thus start with the kink solution and also incorporate the lower bosonic and fermionic shape fluctuation modes.

4.1 Low-energy dynamics of a single vibrating kink

The bosons shape mode in the simplest $g = 2\lambda$ for both kink and antikink, centered either at $a = 1.5$ or $a = -1.5$ are plotted in Figure 1 (left) when $A = 3$. Besides, there is in the simplest $g = 2\lambda$ case, $\nu = 2$, there is only a shape mode of each type, and we focus on the configuration

$$\begin{aligned} \phi(\tau, y) &= \phi_K(y) + A(\tau) \eta_{\sqrt{3}}(y) = \tanh[y - a(\tau)] + A(\tau) \frac{\sinh[y - a(\tau)]}{\cosh^2[y - a(\tau)]}, \\ \frac{1}{\sqrt{g}} \Psi_{\sqrt{3}}(\tau, y, a, \Lambda) &= \Lambda(\tau) \Phi(t, a(\tau)) \simeq \frac{\Lambda(\tau)}{\cosh[y - a(\tau)]} \begin{pmatrix} \tanh[y - a(\tau)] \\ 1/\sqrt{3} \end{pmatrix} \end{aligned}$$

where the kink configuration is supplemented by the bosonic and fermionic shape modes, both of frequency $\Omega = \sqrt{3}$. The space parametrized by the collective coordinates is thus a four-dimensional supermanifold. There are two bosonic collective coordinates, the kink center a and the amplitude of the bosonic shape mode A , spanning the “body.” The “soul” of the submanifold is spanned in turn by one fermionic collective coordinate, the amplitude of the fermionic shape mode: Λ . Now, a very subtle point: in classical field theory, bosonic fields present no problems. Classical Fermi fields are incompatible with the exclusion principle and thus, strictly speaking, do not exist. A loophole to deal with this problem is to focus on the anticommutation rules and look at their classical limit, which is only satisfied by Grassmann variables. It is then natural to consider classical Fermi fields as Grassmann fields, but then, there is no possibility of having the Dirac sea as the ground

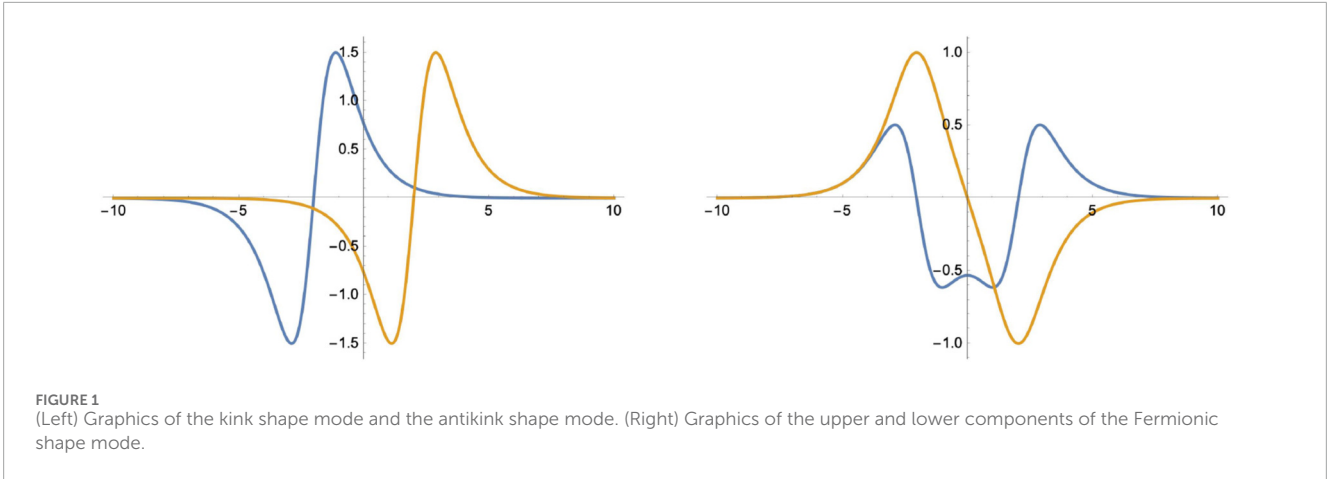


FIGURE 1 (Left) Graphics of the kink shape mode and the antikink shape mode. (Right) Graphics of the upper and lower components of the Fermionic shape mode.

state. One must cope with the existence of spinor waves propagating with negative energy. Within this spirit, we shall consider that the shape mode amplitude, $\Lambda = \Lambda_1 + i\Lambda_2$, is a complex Grassmann variable:

$$\Lambda^2 = 0 = \Lambda^{*2}, \quad \Lambda\Lambda^* + \Lambda^*\Lambda = 0,$$

$$\Lambda_1^2 = 0 = \Lambda_2^2, \quad \Lambda_1\Lambda_2 + \Lambda_2\Lambda_1 = 0, \quad \Lambda^*\Lambda = 2i\Lambda_1\Lambda_2.$$

Under the adiabatic hypothesis, where the temporal dependence of the system is encoded in the collective coordinates $a(\tau)$, $A(\tau)$, $\Lambda(\tau)$, the dynamics is reduced to a finite-dimensional Lagrangian system. The kinetic energy and the potential energy receive contributions from both the bosonic and fermionic collective coordinates. Remembering the vibrating kink configuration

$$\phi_K(y, a, A) = \tanh(y - a) \left(1 + \frac{A}{\cosh(y - a)} \right),$$

and the two components of the Fermionic bound state of energy $\sqrt{3}$, the Fermionic shape mode of fluctuations over the vibrating kink is

$$\psi_{1/\sqrt{3}}^{(2)}(y, a, \Lambda) = \frac{\Lambda}{\cosh(y - a)} {}_2F_1\left(4, -1, 2, \frac{1}{2}(1 + \tanh(y - a))\right) = \Lambda f(y, a)$$

$$\psi_{2/\sqrt{3}}^{(2)}(y, a, \Lambda) = \frac{\Lambda}{\cosh(y - a)} {}_2F_1\left(3, 0, 2, \frac{1}{2}(1 + \tanh(y - a))\right) = \Lambda g(y, a)$$

The contributions due to the bosonic and fermionic shape modes to the effective kinetic and potential energies are⁶

$$T_{\text{eff}}^B = \frac{1}{2} \int_{-\infty}^{\infty} dy \left(\frac{\partial \phi_K}{\partial a} \dot{a} + \frac{\partial \phi_K}{\partial A} \dot{A} \right)^2 = \frac{1}{2} \left[\left(\frac{4}{3} + \frac{\pi}{2} A + \frac{14}{15} A^2 \right) \dot{a} \dot{a} + \frac{2}{3} \dot{A} \dot{A} \right],$$

$$T_{\text{eff}}^F = -\Lambda^* \dot{\Lambda} \int_{-\infty}^{\infty} dy (f[y, a]^2 + g[y, a]^2) + i\Lambda^* \Lambda \int_{-\infty}^{\infty} dy \left[f[y, a] \frac{\partial f}{\partial a} + g[y, a] \frac{\partial g}{\partial a} \right] \dot{a} = -\frac{8}{3} \Lambda^* \Lambda.$$

The effective potential energies due to the bosonic and fermionic collective variables are slightly more difficult to compute:

$$V_{\text{eff}}^B = \frac{1}{2} \int_{-\infty}^{\infty} dy \left(\left(\frac{d\phi}{dy} \right)^2 + (1 - \phi^2)^2 \right) = \left(\frac{4}{3} + A^2 + \frac{\pi}{8} A^3 + \frac{2}{35} A^4 \right),$$

$$V_{\text{eff}}^F = i\Lambda^* \Lambda \int_{-\infty}^{\infty} dy \left[f(y, a) \left(-\frac{d}{dy} + 2\phi_K(y, a, A) \right) g(y, a) + g(y, a) \left(\frac{d}{dy} + 2\phi_K(y, a, A) \right) f(y, a) \right]$$

$$= -i\Lambda^* \Lambda \left(4 + \frac{\pi}{2} A \right) = i\Lambda^* \Lambda \cdot W[a, A]$$

We notice now the main conceptual facts: (1) fluctuations in the kink's center of mass a and the amplitude of vibrating shape modes, both scalar (bosonic) and spinorial (fermionic), are entangled. Thus, if the kink kinetic energy decreases, the frequency of kink oscillations increases. (2) The amplitude of the fermionic fluctuations is coupled to the amplitude of the bosonic ones via a Yukawa interaction between one real and one complex degrees of freedom, remarkably independent of the kink position a . To make these statements more precise, we look at the motion equations derived from the effective Lagrangian

$$L_{\text{eff}} = T_{\text{eff}}^B + T_{\text{eff}}^F - V_{\text{eff}}^B - V_{\text{eff}}^{FB}, \quad L_{\text{eff}}^F = -\frac{4}{3} \Lambda^* \dot{\Lambda} - iW[a, A] \cdot \Lambda^* \Lambda,$$

⁶ Note that the expressions for the fermionic kinetic and potential energies are hermitian due to the anti-hermiticity of $\frac{\partial}{\partial \tau}$ and the anti-commutativity of the Grassmann fields Ψ^\dagger and Ψ .

$$L_{\text{eff}}^B = \frac{1}{2} \left[\left(\frac{4}{3} + \frac{\pi}{2}A + \frac{14}{15}A^2 \right) \dot{a}\dot{a} + \frac{2}{3}\dot{A}\dot{A} \right] + \left(\frac{4}{3} + A^2 + \frac{\pi}{8}A^3 + \frac{2}{35}A^4 \right),$$

which are

$$\frac{d}{d\tau} \left[\left(\frac{4}{3} + \frac{\pi}{2}A + \frac{14}{15}A^2 \right) \dot{a} \right] = i \frac{\partial W}{\partial a} \Lambda^* \Lambda, \tag{24}$$

$$\frac{2}{3}\ddot{A} = \left(\frac{\pi}{2} + \frac{28}{15}A \right) \dot{a}^2 - \left(2A + \frac{3\pi}{8}A^2 + \frac{8}{25}A^3 \right) - i \frac{\partial W}{\partial A} \Lambda^* \Lambda, \tag{25}$$

$$i\dot{\Lambda}^* = W[a, A] \cdot \Lambda^*. \tag{26}$$

Consider first the situation where the fermionic fluctuations are null: $\Lambda(\tau) = 0, \forall \tau$. Then, the first of the Euler–Lagrange (EL) equations gives rise to a constant of motion because a is a cyclic variable:

$$\left(\frac{4}{3} + \frac{\pi}{2}A + \frac{14}{15}A^2 \right) \dot{a} = C \equiv \dot{a} = \frac{C}{\frac{4}{3} + \frac{\pi}{2}A + \frac{14}{15}A^2}.$$

Still in the absence of fermionic fluctuations, and focusing on the regime of small shape mode amplitude, the second motion equation becomes linear

$$\begin{aligned} \ddot{A} &\simeq D(C) - \omega^2(C)A + \mathcal{O}(A^2), & D(C) &= \frac{9\pi}{32}C^2, \\ \omega^2(C) &= 3 - \left(\frac{21}{20} - \frac{27\pi^2}{256}C^2 \right). \end{aligned}$$

Having chosen the $\Lambda = 0 = \Lambda^*$ solution of the motion equations for the Grassmann degree of freedom, the main impact of the shape mode in the kink dynamics is clearly shown. The frequency of the kink oscillations is modified as a function of $C \propto \dot{a}$. That is, the faster the vibrating kink moves, the lower its oscillation frequency becomes and vice versa. This transference from kinetic to potential energy in kink dynamics is a semi-classical effect because the shape mode appears at order \hbar in the \hbar expansion of the Jackiw–Rebbi action. The dependence of the shape mode amplitude on time is easily recognized if fermionic fluctuations do not enter the game:

$$A(\tau) = \frac{D(C)}{\omega^2(C)} + \mathcal{A}(\cos(\omega(C)\tau) + \mathcal{D}).$$

We stress that there is a critical value of C . If $|C| > 2\sqrt{\frac{5}{7}}$ $\omega(C)$ becomes imaginary, and the kink stops oscillating, the evolution is purely kinetic. When $|C| < 2\sqrt{\frac{5}{7}}$, the translational and vibrational movements coexist. Any perturbation producing a variation of C produces a variation of the shape mode frequency and vice versa, just qualitatively agreeing with the numerical predictions in the full field theoretical model.

The mutual influence between bosonic and fermionic fluctuations is understood if we consider the dynamics determined by the third equation. Equation 26 reads

$$i\dot{\Lambda}^*(\tau) = -\left(4 + \frac{\pi}{2}A \right) \Lambda^*. \tag{27}$$

The formal solution is easy to find:

$$\Lambda^*(\tau) = \delta^* \exp \left[i \frac{1}{2} \int_0^\tau d\tau' \left(4 + \frac{\pi}{2}A(\tau') \right) \right], \tag{28}$$

where $\delta^* = \delta_1 - i\delta_2, \delta_1^2 = \delta_2^2 = 0$, is a Grassmann integration constant. Thus, $i\Lambda^*(\tau)\Lambda(\tau) = i\delta^* \delta$, and therefore,

$$\begin{aligned} \ddot{A} &\simeq D(C) - 2 \cdot i\delta^* \delta - \left(\omega^2(C) - i \frac{\pi}{2} \delta^* \delta \right) A + \mathcal{O}(A^2) \implies, \\ A(\tau) &\simeq \frac{D(C) - 2 \cdot i\delta^* \delta}{\omega^2(C) - i \frac{\pi}{2} \delta^* \delta} + \mathcal{A} \left(\cos \left(\left(\omega(C) - i \frac{\pi}{2} \delta^* \delta \right) \tau \right) + \mathcal{D} \right). \end{aligned}$$

The spinorial kink fluctuations interact with the scalar kink fluctuations, modifying the midpoint of the scalar fluctuation amplitudes and the vibration frequencies.

In order to calibrate how the kink dynamics depends on the oscillatory shape modes also for $\frac{\xi}{\lambda} = 3$, let us consider the two vibrating modes. The spinor fields describing these oscillations are

$$\begin{aligned} \Psi_{\sqrt{5}}^{(1)}(\tau, y, a) &= \Lambda(\tau) \Phi^{(1)}(y, a) = \frac{\Lambda(\tau)}{\cosh^2(y - a(\tau))} \begin{pmatrix} {}_2F_1 \left(6, -1, 3, \frac{1}{2} (1 + \tanh(y - a(\tau))) \right) \\ {}_2F_1 \left(5, 0, 3, \frac{1}{2} (1 + \tanh(y - a(\tau))) \right) \end{pmatrix}, \\ \Psi_{\sqrt{8}}^{(2)}(\tau, y, a) &= \Lambda(\tau) \Phi_{\sqrt{8}}^{(2)}(y, a) = \frac{\Lambda(\tau)}{\cosh(y - a(\tau))} \begin{pmatrix} {}_2F_1 \left(5, -2, 2, \frac{1}{2} (1 + \tanh(y - a(\tau))) \right) \\ {}_2F_1 \left(4, -1, 2, \frac{1}{2} (1 + \tanh(y - a(\tau))) \right) \end{pmatrix}. \end{aligned}$$

Only the Fermionic kinetic and potential energies are modified because, even though $g/\lambda = 3$, we stick to the standard ϕ^4 kink:

$$\begin{aligned} T_{\text{eff}}^{F(1)} &= -\Lambda^* \dot{\Lambda} \int_{-\infty}^{\infty} dy \left(\Phi^{T(1)}(y) \Phi^{(1)}(y) \right) = -\frac{8}{5} \Lambda^* \dot{\Lambda}, \\ T_{\text{eff}}^{F(2)} &= -\Lambda^* \dot{\Lambda} \int_{-\infty}^{\infty} dy \left(\Phi^{T(2)}(y) \Phi^{(2)}(y) \right) = -\Lambda^* \dot{\Lambda}, \\ V_{\text{eff}}^{F(1)} &= i\Lambda^* \Lambda \int_{-\infty}^{\infty} dy \Phi^{T(1)}(y) \left(-i\sigma_2 \frac{d}{dy} + 3\sigma_1 \tanh y \left(1 + \frac{A}{\cosh y} \right) \right) \Phi^{(1)}(y) = -i\Lambda^* \Lambda \left(\frac{8}{3} + \frac{3\pi}{8} A \right), \\ V_{\text{eff}}^{F(2)} &= i\Lambda^* \Lambda \int_{-\infty}^{\infty} dy \Phi^{T(2)}(y) \left(-i\sigma_2 \frac{d}{dy} + 3\sigma_1 \tanh y \left(1 + \frac{A}{\cosh y} \right) \right) \Phi^{(2)}(y) = -i\Lambda^* \Lambda \left(\frac{8}{3} + \frac{21}{64} A \right). \end{aligned}$$

Therefore, the effective models are Lagrangian dynamical systems where the configuration spaces are supermanifolds. The dynamical variables are both c -numbers, a and A , and Grassmann magnitudes, Λ^* and Λ . The fact that the effective super dynamical systems are not super symmetric is due to the property that shape modes are not Bogomol'nyi–Prasad–Sommerfield (BPS) bound. *Although we started with no backreaction of the fermions on the kink at the classical level, this effect arises at the one-loop level by taking into account the effect of fermionic shape modes.*

4.2 Effective dynamics of vibrating kink–antikink configurations

4.2.1 Effective kinetic energy

The kink–antikink configurations depend on two parameters when the two basic topological defects are vibrating:

$$\begin{aligned} \phi_{KA}(y, a(\tau), A(\tau)) &= \tanh(a(\tau) + y) - \tanh(y - a(\tau)) - 1 \\ &+ \frac{A(\tau)}{\tanh(a(\tau))} (\tanh(a(\tau) + y) \cdot \text{sech}(a(\tau) + y) - \tanh(y - a(\tau)) \cdot \text{sech}(a(\tau) - y)), \end{aligned} \tag{29}$$

where a labels the relative position of the kink with respect to the antikink, and A labels the synchronized amplitudes of vibrating kink and antikink. It is assumed that the center of mass is placed at the origin of the reference system.

In Equation 29, the adiabatic approximation is implemented: only the collective coordinates a and A depend on the τ time. The evolution is so smooth that the spatial coordinate y remains constant in time. Under this hypothesis, a non-Euclidean metric arises in the (a, A) plane:

$$\begin{aligned} g_{aa}(a, A) &= \int_{-\infty}^{\infty} dy \left(\frac{\partial \phi_{KA}}{\partial a} \cdot \frac{\partial \phi_{KA}}{\partial a} \right), \quad g_{aA}(a, A) = \int_{-\infty}^{\infty} dy \left(\frac{\partial \phi_{KA}}{\partial a} \cdot \frac{\partial \phi_{KA}}{\partial A} \right), \\ g_{AA}(a, A) &= \int_{-\infty}^{\infty} dy \left(\frac{\partial \phi_{KA}}{\partial A} \cdot \frac{\partial \phi_{KA}}{\partial A} \right), \quad \dot{a} = \frac{\partial a}{\partial \tau}, \quad \dot{A} = \frac{\partial A}{\partial \tau}, \end{aligned}$$

such that the kinetic energy of the kink–antikink adiabatic evolution becomes

$$T_{\text{eff}}^{KA} = \frac{1}{2} \left(g_{aa}(a, A) \dot{a}^2 + 2g_{aA}(a, A) \dot{a} \dot{A} + g_{AA}(a, A) \dot{A}^2 \right).$$

Computations with Mathematica offer the following results:

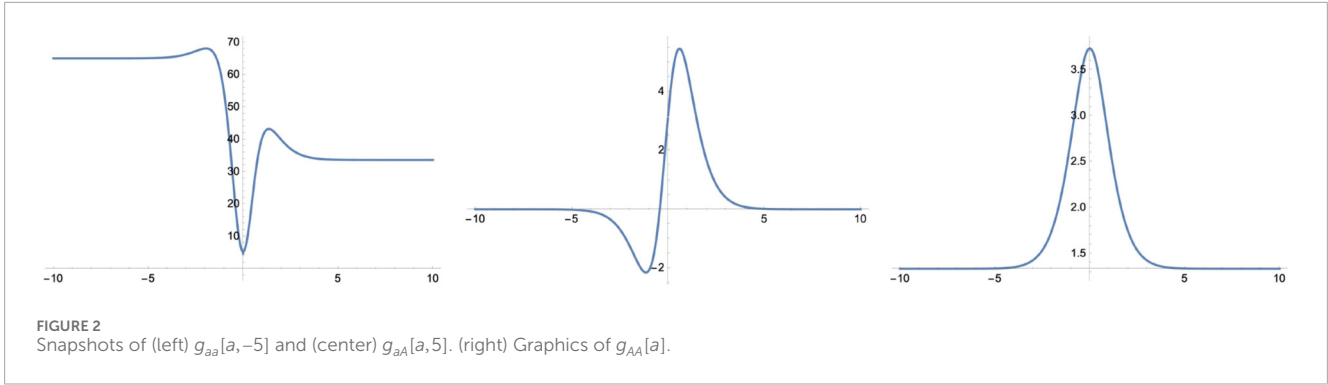
$$\begin{aligned} g_{aa}(a, A) &= \frac{480ae^{10a} (A^2 \cosh(8a) + 4(46A^2 + 7) \cosh(2a) + 4(23A^2 - 4) \cosh(4a) + 4(2A^2 + 1) \cosh(6a) + 163A^2 - 16)}{15(e^{2a} - 1)^7 (e^{2a} + 1)^3} \\ &- \frac{16e^{10a} \sinh(2a) (40(93A^2 - 13) \cosh(2a) + (668A^2 + 80) \cosh(4a) + 40(3A^2 + 1) \cosh(6a))}{15(e^{2a} - 1)^7 (e^{2a} + 1)^3} \\ &- \frac{16e^{10a} \sinh(2a) ((7A^2 + 10) \cosh(8a) + 2219A^2 + 410) + 15\pi(e^{2a} - 1)^{10} A}{15(e^{2a} - 1)^7 (e^{2a} + 1)^3}, \end{aligned}$$

$$\begin{aligned} g_{aA}(a, A) &= -A \tanh(a) - 5A \text{Acsch}^6(a) - 7A \text{Acsch}^4(a) - 3A \text{Acsch}^2(a) + (\pi - aA) \text{sech}^2(a) \\ &+ \coth(a) \left(5A \text{Acsch}^4(a) + \frac{11}{3} A \text{Acsch}^2(a) + A \right), \end{aligned}$$

$$g_{AA}(a) = \frac{1}{24} \text{csch}^5(a) \text{sech}(a) (36a - 3 \sinh(2a) - 12 \sinh(4a) + \sinh(6a) + 12a \cosh(4a)).$$

Starting with the aa component of the metric tensor, we observe that the limits when a tends to $\pm\infty$ are

$$\lim_{a \rightarrow \pm\infty} g_{aa}[a, A] = \frac{8}{3} \pm \pi A + \frac{28}{15} A^2.$$



These limits correspond to infinite separation between the kink and antikink centers, the antikink at the right with respect to the kink, the + sign, or vice versa, the - sign. Clearly, this component of the metric tensor is twice the metric of one excited single kink. Near the origin, the aa component metric tensor behaves as follows:

$$g_{aa}[a, A] \simeq_{a \rightarrow 0} \pi a^3 A + a^2 \left(\frac{248A^2}{63} - \frac{64}{15} \right) + \frac{16}{3}.$$

The limits of the other components of the metric tensor at $\pm\infty$ are

$$\lim_{a \rightarrow \pm\infty} g_{aA}[a, A] = 0, \quad \lim_{a \rightarrow \pm\infty} g_{AA}[a, A] = \frac{4}{3},$$

confirming that when kink-antikink are very far apart, they behave as two isolated single kinks, and their interactions are negligible. Close to the origin, when the kink and antikink are superposed, these components of the metric tensor become

$$g_{aA}[a, A] \simeq_{a \rightarrow 0} -\pi a \left(\frac{152}{105} A + a \right) + \frac{80}{63} A a^3, \quad g_{AA}[a, A] \simeq_{a \rightarrow 0} \frac{56}{15} - \frac{152}{105} a^2.$$

In Figure 2 plots of the metric tensor induced by the bosons shape modes on kink-anti kink configurations, $g_{aa}[a, -5]$, $g_{aa}[a, 5]$ and $g_{AA}[a]$, are shown as functions of a .

4.2.2 Effective potential energy

The last step is the computation of the effective potential energy between vibrating kink and antikink topological defects in the adiabatic regime of collective coordinates:

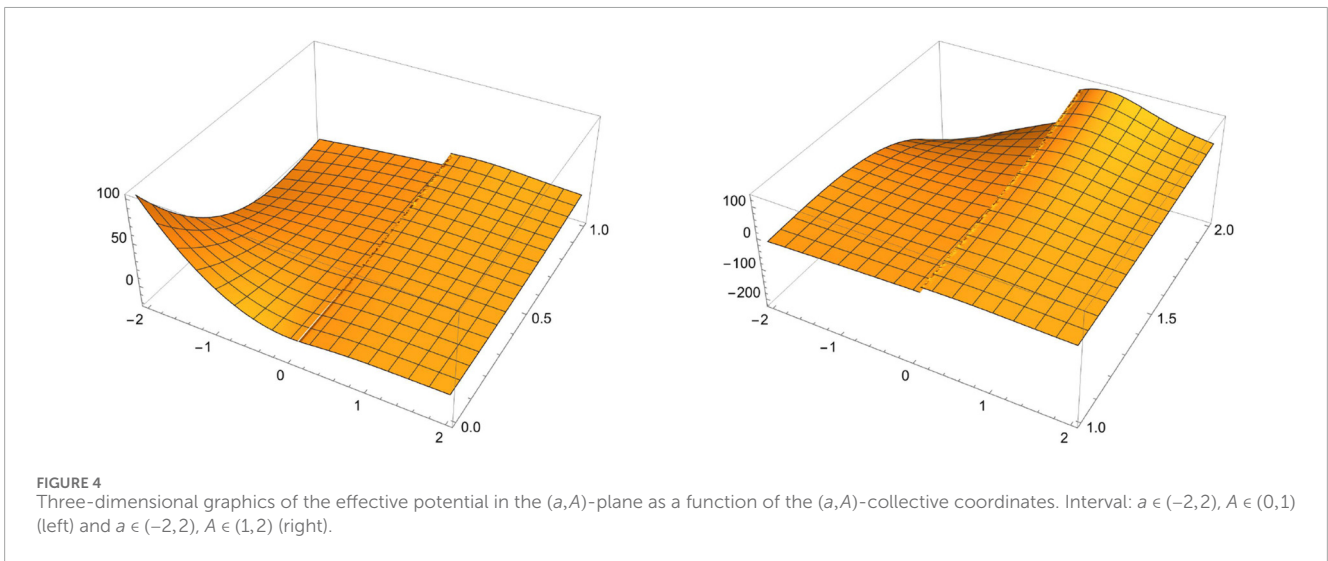
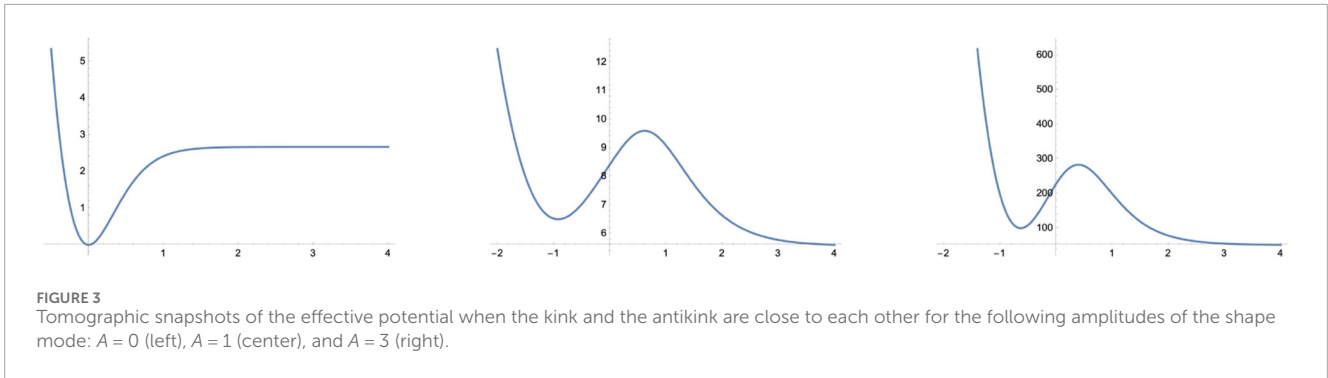
$$V_{\text{eff}}^{KA}[a, A] = \frac{1}{2} \int_{-\infty}^{\infty} dy \left(\frac{\partial \phi_{KA}}{\partial y} \cdot \frac{\partial \phi_{KA}}{\partial y} + (1 - \phi_{KA}^2(y, a, A))^2 \right). \tag{30}$$

The calculation requires a huge computational effort, and here is the result achieved in a Mathematica environment:

$$V_{\text{eff}}^{KA}[a, A] = \frac{1}{210(e^{2a} - 1)^{11}(e^{2a} + 1)^3} \times \left\{ \frac{105}{2} \pi (e^{2a} - 1)^{11} A \left((-141e^{2a} + 45e^{4a} + e^{6a} - 1) A^2 + 96(e^{2a} - 1) \right) \right. \\ + 16(e^{4a} - 1) 3e^{12a} A^4 (10696 \cosh(2a) - 15105 \cosh(4a) + 2716 \cosh(6a) - 986 \cosh(8a) + 28 \cosh(10a) + \cosh(12a) - 17510) \\ - 840e^{12a} A^2 \sinh^4(a) (-288 \sinh(2a) + 40 \sinh(4a) - 96 \sinh(6a) + 4 \sinh(8a)) \\ + 656 \cosh(2a) - 124 \cosh(4a) + 112 \cosh(6a) - 5 \cosh(8a) - 159 + (35(-8e^{4a} + e^{8a} - 17)(e^{2a} - 1)^8 \\ + 1680a(8e^{11a}(3e^{3a}A^4(130 \cosh(2a) - 32 \cosh(4a) + 29 \cosh(6a) - 4(\cosh(8a) + 7) + \cosh(10a)) \\ + 12e^{3a}A^2 \sinh^4(a)(8 \sinh(2a) - 80 \sinh(4a) + 8 \sinh(6a) - 8 \sinh(8a)) \\ - 80 \cosh(2a) + 124 \cosh(4a) - 16 \cosh(6a) + 9 \cosh(8a) + 123) \\ + 11(42 \sinh(a) - 5(6 \sinh(3a) - 3 \sinh(5a) + \sinh(7a)) + \sinh(9a)) \\ \left. + 14 \cosh(a) - 22 \cosh(3a) + 5 \cosh(5a) + 7 \cosh(7a) - 5 \cosh(9a) + 8 \right\}.$$

Close to the origin, the effective kink-antikink potential behaves as

$$V_{\text{eff}}^{KA}[a, A] \simeq_{a \rightarrow 0} \frac{1}{420} a^3 (-3255\pi A^3 + 11520A^2 + 1680\pi A - 7168) \\ + \frac{a^2 (-94912A^4 + 45045\pi A^3 + 322036A^2 - 180180\pi A + 192192)}{15015} \\ + \frac{2}{35} a (105\pi A^3 - 608A^2 + 105\pi A) + \frac{5152A^4 - 3465\pi A^3 + 15444A^2}{1155}.$$



Special values of the effective potential at distinguished points are

$$\lim_{a \rightarrow 0} V_{\text{eff}}^{KA}[a, A] = \frac{736A^4}{165} - 3\pi A^3 + \frac{468A^2}{35}, \quad \lim_{a \rightarrow \infty} V_{\text{eff}}^{KA}[a, A] = \frac{8}{3} + \frac{\pi}{4}A^3 + \frac{4}{35}A^4, \quad \lim_{a \rightarrow -\infty} V_{\text{eff}}^{KA}[a, A] = \infty.$$

The qualitative properties of this mechanical potential are encoded in Figures 3, 4.

If both kink and antikink are non-excited, that is, when $A = 0$, the low-energy dynamics is captured by a Lagrangian mechanical system with a single degree of freedom, the relative position a :

$$L = \frac{1}{2}g[a, 0]\dot{a}\dot{a} - V_{\text{eff}}^{KA}[a, 0].$$

Therefore, the system is Liouville integrable and, because the energy

$$E = \frac{1}{2}g[a, 0]\dot{a}\dot{a} + V_{\text{eff}}^{KA}[a, 0]$$

is a constant of motion, it is possible to reduce the integration of the system to a quadrature:

$$t - t_0 = \int da \sqrt{\frac{g[a, 0]}{2(E - V_{\text{eff}}^{KA}[a, 0])}}. \tag{31}$$

It is not possible, either by writing the integral in terms of analytical functions or, even if it not were the case, to invert the outcome and to know the explicit dependence of a on time. Nevertheless, Figure 3 (left), as well as the explicit knowledge of $V_{\text{eff}}^{KA}[a, 0]$, makes possible a qualitative analysis of the motion. $E = \frac{8}{3}$ is the threshold for unbounded motion, and bounded motion occurs if $0 < E < \frac{8}{3}$. Thus, for energies greater than $\frac{8}{3}$, starting with initial conditions $(a(t - t_0 \ll 0) \gg 0, \dot{a}(t - t_0 \ll 0) < 0)$ a decreases when times runs forward until it becomes slightly negative, meaning that kink and antikink centers cross each other while exchanging their relative position. For sufficiently high energy, the relative position a becomes sufficiently negative to reach the infinite potential barrier sooner or later. Then, a bounce is produced, and a second exchange between kink and antikink takes place, moving the KAK pair apart, again up to very long distances. For energies less

than $\frac{8}{3}$ but greater than 0, the kink–antikink motion is bounded. These oscillatory motions were christened as “bions” by their discoverers in [15, 16]. In Figure 5 we plot both the induced metric and the effective potential due to the sermonic shape mode with the highest frequency of the kink–anti kink configuration when $g = 3\lambda$. The plots of the effective potentials for $A01$ and $A = 3$, Figure 3 (center) and (right) show a similar pattern, but less room for bions is left with increasing shape mode amplitudes.

A brief digression on the quantum description of the previously described classical dynamics is convenient. Because the momentum conjugate to a is $p_a = g[a, 0]\dot{a}$, the quantum momentum operator becomes $\hat{p}_a = -i\frac{d}{da}$, while the quantum Hamiltonian, Weyl ordered, reads:

$$\hat{H} = -\frac{1}{\sqrt{g[a, 0]}} \frac{d}{da} \left(\sqrt{g^{-1}[a, 0]} \frac{d}{da} \right) - V_{\text{eff}}^{KA}[a, 0]. \tag{32}$$

The unbounded motion orbits become scattering backward waves while bound states arise from the bounded orbits, only complying with some Bohr–Sommerfeld quantization conditions.

If both kink and antikink are excited, and we let the amplitude A vary, things are different. The effective dynamics is captured by a Lagrangian system with two degrees of freedom: a and A . Denoting now $a = a^1$ and $A = a^2$, the effective Lagrangian reads

$$L = \frac{1}{2} g_{a^i a^j}[a^1, a^2] \frac{\partial a^i}{\partial \tau} \cdot \frac{\partial a^j}{\partial \tau} - V_{\text{eff}}^{KA}[a^1, a^2], \quad i, j = 1, 2,$$

and, accordingly, the motion equations become

$$\frac{\partial^2 a^i}{\partial \tau^2} + \sum_{j,k} \Gamma_{a^i a^k}^{a^j} \frac{\partial a^j}{\partial \tau} \frac{\partial a^k}{\partial \tau} = - \sum_j g^{a^i a^j} \frac{\delta V}{\delta a^j}, \quad \Gamma_{a^i a^k}^{a^j} = \frac{1}{2} \sum_l g^{a^l a^l} \left(\frac{\partial g_{a^i a^j}}{\partial a^k} + \frac{\partial g_{a^l a^k}}{\partial a^i} - \frac{\partial g_{a^l a^i}}{\partial a^k} \right).$$

The energy is still a constant of motion, but there is no second invariant that would guarantee the Liouville integrability of the system. Needless to say, obtaining analytical solutions of this system of ordinary differential equations (ODEs) is hopeless. Nevertheless, numerical analysis of this system for initial conditions corresponding to kink–antikink scattering has been successfully performed in the seminal [4]. These authors reached a similar conclusion to those previously obtained in the numerical treatment of the full field theory: in the kink–antikink scattering, quasi-bound states where several bounces occur arise for some windows of initial velocities. Moreover, the pattern shows a very interesting fractal structure.

4.3 Fermionic fluctuations of kink–antikink configurations

Consider the bounded spinorial fluctuation over the kink–antikink configuration when the ratio $\frac{g}{\lambda}$ is 2.

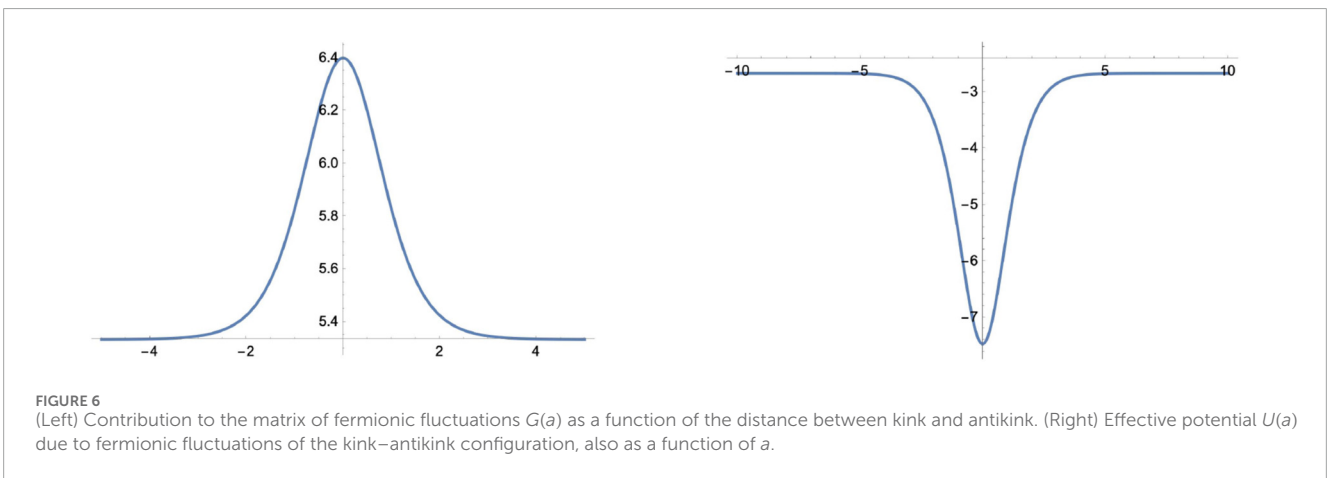
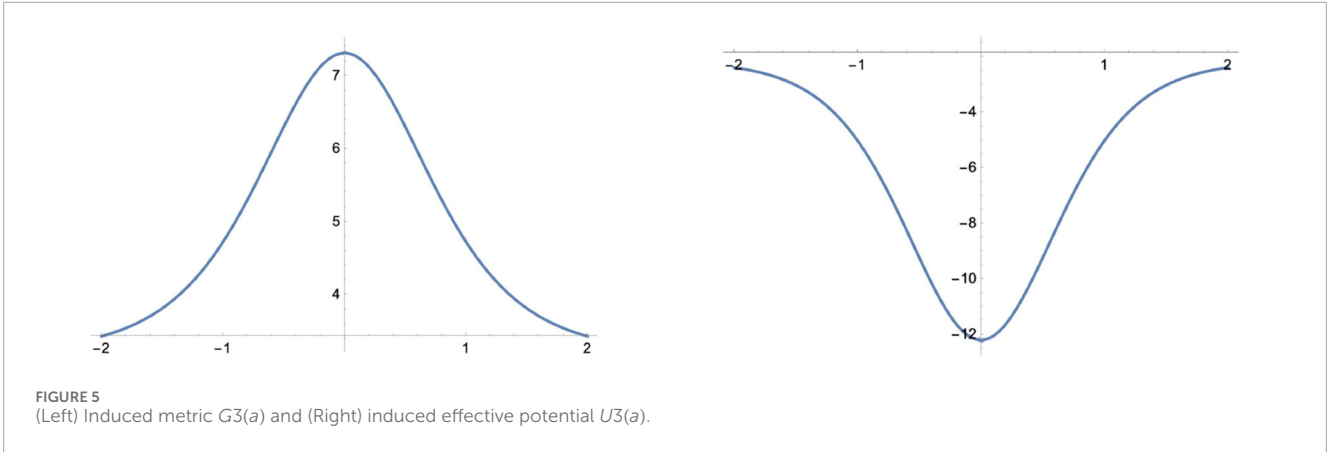
$$\frac{1}{\sqrt{g}} \Psi_{\sqrt{3}\sqrt{3}}(y, a, \Lambda) = \frac{\Lambda}{\tanh[a]} \times \left[\text{sech}(y+a) \begin{pmatrix} 2F_1\left(4, -1, 2, \frac{1}{2}(1 + \tanh(y+a))\right) \\ 2F_1\left(3, 0, 2, \frac{1}{2}(1 + \tanh(y+a))\right) \end{pmatrix} \right. \\ \left. - \text{sech}(y-a) \begin{pmatrix} 2F_1\left(4, -1, 2, \frac{1}{2}(1 + \tanh(y-a))\right) \\ 2F_1\left(3, 0, 2, \frac{1}{2}(1 + \tanh(y-a))\right) \end{pmatrix} \right] \tag{33}$$

In Figure 1 (right) the upper (blue) and the lower (yellow) components of the sermonic shape mode on kink–anti kink configurations are drawn as functions of a when the distance between centers is $a = 2$. Contribution to the kinetic energy of the fermionic fluctuations

$$T_{\text{eff}}^F = - \int_{-\infty}^{\infty} dy \Psi_{\sqrt{3}\sqrt{3}}^\dagger(y, a, \Lambda) \Psi_{\sqrt{3}\sqrt{3}}(y, a, \Lambda) = -\Lambda^* \Lambda G(a), \\ G(a) = \frac{1}{\tanh^2 a} \int_{-\infty}^{\infty} dy \left[\left(\frac{\tanh(y+a)}{\cosh(y+a)} - \frac{\tanh(y-a)}{\cosh(y-a)} \right)^2 + (\text{sech}(y+a) - \text{sech}(y-a))^2 \right] \\ = \frac{4}{3} (12a - 3 \sinh(2a) - 3 \sinh(4a) + \sinh(6a)) \coth^2(a) \text{csch}^3(2a). \tag{34}$$

Next, we compute the effective potential contributed by the fermionic shape mode fluctuating over the kink–antikink configuration:

$$V_{\text{eff}}^F(a, \Lambda^* \Lambda) = i \int_{-\infty}^{\infty} dy \Psi_{\sqrt{3}\sqrt{3}}^\dagger(y, a, \Lambda) \left\{ -i\sigma_2 \frac{d}{dy} + 2\phi_{KA}(y, a, A) \right\} \Psi_{\sqrt{3}\sqrt{3}}(y, a, \Lambda) = i\Lambda^* \Lambda \cdot U(a), \\ U(a) = \frac{1}{\tanh^2 a} \int_{-\infty}^{\infty} dy \left[\left(\frac{{}_2F_1\left[4, -1, 2, \frac{1}{2}(1 + \tanh(y+a))\right]}{\cosh(y+a)} - \frac{{}_2F_1\left[4, -1, 2, \frac{1}{2}(1 + \tanh(y-a))\right]}{\cosh(y-a)} \right) \right. \\ \times \left(-\frac{d}{dy} + 2\phi_{KA}(y, a, A) \right) \left(\frac{{}_2F_1\left[3, 0, 2, \frac{1}{2}(1 + \tanh(y+a))\right]}{\cosh(y+a)} - \frac{{}_2F_1\left[3, 0, 2, \frac{1}{2}(1 + \tanh(y-a))\right]}{\cosh(y-a)} \right) \\ \left. + \left(\frac{{}_2F_1\left[3, 0, 2, \frac{1}{2}(1 + \tanh(y+a))\right]}{\cosh(y+a)} - \frac{{}_2F_1\left[3, 0, 2, \frac{1}{2}(1 + \tanh(y-a))\right]}{\cosh(y-a)} \right) \right. \\ \left. \times \left(\frac{d}{dy} + 2\phi_{KA}(y, a, A) \right) \left(\frac{{}_2F_1\left[4, -1, 2, \frac{1}{2}(1 + \tanh(y+a))\right]}{\cosh(y+a)} - \frac{{}_2F_1\left[4, -1, 2, \frac{1}{2}(1 + \tanh(y-a))\right]}{\cosh(y-a)} \right) \right],$$



where $\phi_{KA}(y, a, A)$ is the excited kink–antikink configuration defined in Equation 29. The result is

$$U(a) = -\frac{2}{3} \coth^2(a) \operatorname{csch}^3(2a) (\log(e^{36a}) - 3 \sinh(2a) - 12 \sinh(4a) + \sinh(6a) + 6 \log(e^{2a}) \cosh(4a)) . \tag{35}$$

Because the fermionic kink–antikink fluctuations do not depend on the shape mode vibration amplitude of kink and antikink, we expect that $G(a)$ only will be a function of a , and indeed, this is the case. The effective potential $U(a)$ induced by the fermionic fluctuations on vibrating kink–antikink configurations, however, does not depend on the amplitude of the bosonic shape mode. This unexpected effect is due to the fact (see Figure 6 (left)) that kink and antikink oscillate in counter-phase, and there is destructive interference. Thus, one should expect that interactions between the amplitudes Λ and A , respectively, of fermionic and bosonic fluctuations of kink–antikink configurations only would arise if the amplitudes of vibrations of the kink differ from the antikink amplitudes. To test this statement, generalization to consider the amplitude of the kink different from the antikink amplitude in the shape modes is implemented by replacing in the kink–antikink configuration the contribution of excitations by

$$A \frac{\tanh(y+a)}{\cosh(y+a)} - B \frac{\tanh(y-a)}{\cosh(y-a)} .$$

A quick Mathematica run confirms the conceptual argument given above:

$$U(a, A - B) = -\frac{\coth^2(a) \left(\frac{3}{2} \pi (e^{2a} - 1)^6 (A - B) + 16e^{6a} (36a - 3 \sinh(2a) - 12 \sinh(4a) + \sinh(6a) + 12a \cosh(4a)) \right)}{3(e^{4a} - 1)^3} .$$

Understanding how the induced metric and effective potential by fermionic kink fluctuations depend on $\frac{g}{\lambda}$ starts by looking at $N = 3$. In this case, there are two fermionic shape modes. The lower frequency is $\sqrt{5}$, which, implemented on the excited kink–antikink configuration,

gives rise to the spinor wave function:

$$\frac{1}{\sqrt{g}} \Psi_{\sqrt{5}\sqrt{5}}(y, \Lambda) = \frac{\Lambda}{\tanh a} \left(\frac{{}_2F_1\left[6, -1, 3, \frac{1}{2}(1 + \tanh(y + a))\right]}{\cosh^2(y + a)} - \frac{{}_2F_1\left[6, -1, 3, \frac{1}{2}(1 + \tanh(y - a))\right]}{\cosh^2(y - a)} \right) \quad (36)$$

The effective kinetic energy induced by this fermionic shape mode is

$$T_{\text{eff}}^{F1} = \int_{-\infty}^{\infty} dy \Psi_{\sqrt{5}\sqrt{5}}^\dagger(y, \Lambda) \dot{\Psi}_{\sqrt{5}\sqrt{5}}(y, \Lambda) = -\Lambda^* \dot{\Lambda} \cdot G3(a)$$

$$G3(a) = \frac{1}{5} \coth^2(a) \operatorname{csch}^5(2a) (-80 \sinh(2a) - 15 \sinh(6a) + \sinh(10a) + 120 \log(e^{2a}) \cosh(2a)). \quad (37)$$

Likewise, the effective potential is derived via similar procedures:

$$V_{\text{eff}}^{F1} = i \int_{-\infty}^{\infty} dy \Psi_{\sqrt{5}\sqrt{5}}^\dagger(y, \Lambda) \left\{ -i\sigma_2 \frac{d}{dy} + 3\phi_{KA}(y, a, A) \right\} \Psi_{\sqrt{5}\sqrt{5}}(y, \Lambda) = i\Lambda^* \Lambda \cdot U3(a),$$

$$U3(a) = -\frac{2}{15} \coth^2(a) \operatorname{csch}^5(2a) (-350 \sinh(2a) - 125 \sinh(6a) + \sinh(10a) + 60 \log(e^{2a}) (11 \cosh(2a) + \cosh(6a))).$$

In sum, an identical pattern is observed in the effective adiabatic dynamics induced by fermionic kink shape modes in kink–antikink configurations when $N = 2$ or $N = 3$. We thus omit writing the results obtained for the fermionic shape mode of frequency $\sqrt{8}$, which are qualitatively equivalent but even more cumbersome.

5 Outlook

The theoretical developments in this work have been focused on a field theory (1 + 1)-dimensional model of bosons and fermions, specifically the Jackiw–Rebbi model introduced in [5]. One interesting way to extend these ideas is to increase the number of fields, both bosonic and fermionic. An early proposal in this line can be found in an article published circa 2000 by one MIT group; see [14]. In that work, the authors consider a field theory model with two Bose and two Fermi fields. The interaction between bosonic and fermionic fields is through two Yukawa couplings, and sophisticated phenomena arise. We intend, however, to extend scalar/Bose two-field models treated by our group in Salamanca by incorporating two spinor/Fermi fields into these systems. The first model that we have in mind was discussed, among other articles, in [17]. This field theoretical model exhibits a wide variety of kinks and possesses interesting properties of integrability in the related mechanical analogous system. We expect that when adding spinor/Fermi fields, similar phenomena to those found in the Jackiw–Rebbi model will be kept, but subtle novelties will probably appear. The second system where we envisage that the analysis developed in the JR model will be fruitful is the massive non-linear S^2 -sigma 1 + 1-dimensional model [18]. Again, a manifold of topological and non-topological kinks exists in this “deformed” non-linear sigma model. Spinor/Fermi fields will be included as sections of one spinor bundle over the two-sphere rather than spinor functions. In any case, we expect that new phenomena will appear with respect to those described in the JR model. The interplay between scalar and spinor fields in this non-linear system promises the appearance of new subtleties.

Another playground where the analysis of effective low-energy dynamics seems to be promising is the moduli space of BPS vortices in the Abelian Higgs model; see, for example, [?] for a parallel study devoted to kinks. The Abelian Higgs model in (2 + 1) space-time, at the critical ratio between the self-interacting scalar λ and the electromagnetic e^2 couplings, the transition point between Type I and Type II Ginzburg–Landau superconductivity, possesses manifolds of topological non-interacting stable BPS vortices characterized by an integer number of magnetic quanta. These topological defects also admit vibrational modes; see [19, 20]. The collective coordinate low-energy analysis has been developed in [21–23] in the absence of fermions. The addition of fermions to the Abelian Higgs model is compelling, including Yukawa and electromagnetic couplings. The system will be much more complex, but the temptation is strong toward identifying the collective coordinates of these planar topological defects and seeing how fermions affect the adiabatic dynamics of BPS vortices.

Data availability statement

The original contributions presented in the study are included in the article/Supplementary Material; further inquiries can be directed to the corresponding author.

Author contributions

JG: Conceptualization, Investigation, Software, Writing – original draft.

Funding

The author(s) declared that financial support was not received for this work and/or its publication.

Conflict of interest

The author(s) declared that this work was conducted in the absence of any commercial or financial relationships that could be construed as a potential conflict of interest.

Generative AI statement

The author(s) declared that generative AI was not used in the creation of this manuscript.

Any alternative text (alt text) provided alongside figures in this article has been generated by Frontiers with the support of artificial intelligence and reasonable efforts have been made to ensure accuracy, including review by the authors wherever possible. If you identify any issues, please contact us.

Publisher's note

All claims expressed in this article are solely those of the authors and do not necessarily represent those of their affiliated organizations, or those of the publisher, the editors and the reviewers. Any product that may be evaluated in this article, or claim that may be made by its manufacturer, is not guaranteed or endorsed by the publisher.

References

- Alonso-Izquierdo A, Miguelez-Caballero D, Nieto LM, Queiroga-Nunes J. Wobbling kinks in a two-component scalar field theory: interaction between shape modes. (2023).
- Alonso-Izquierdo A, Nieto LM, Queiroga-Nunes J. Asymmetric scattering between kinks and wobblers. *Comm Nonl Sci Num Sim* (2022) 107:106183. doi:10.1016/j.cnsns.2021.106183
- Alonso-Izquierdo A, Nieto LM, Queiroga-Nunes J. Scattering between wobbling kinks. *Phys Rev* (2021) D103:045003.
- Manton NS, Olés K, Romanczukiewicz T, Wereszczynski A. Collective coordinates model of kink-antikink collisions in ϕ^4 theory. *Phys Rev Lett* (2021) 127:071601.
- Jackiw R, Rebbi C. Solitons with fermion number. *Phys Rev* (1976) D13:3398–409. doi:10.1103/physrevd.13.3398
- Jackiw R, Schrieffer R. Solitons with fermionic number in condensed matter physics and relativistic field theory. *Nucl Phys* (1981) B190:253–332.
- Niemi A, Semenoff GW. Fermion number fractionization in quantum field theory. *Phys Rep* (1986) 135:99–193. doi:10.1016/0370-1573(86)90167-5
- Alonso-Izquierdo A, Fresneda R, Mateos Guilarte J, Vassilevich D. Soliton fermionic number from the heat kernel expansion. *Eur Phys J* (2019) C79:525. doi:10.1140/epjc/s10052-019-7041-8
- Chu Y, Vachaspati T. Fermions on one or fewer Kinks. *Phys Rev* (2008) D77:025006. doi:10.1103/physrevd.77.025006
- Bazeia D, Mohammadi A. Fermionic bound states in distict kinlike backgrounds. *Eur Phys J* (2017) C77:203.
- Campos J, Mohammadi A. Kink-antikink collisions in the supersymmetric ϕ^4 model (2022).
- Bazeia D, Campos J, Mohhamadi A. Resonance mediated by fermions in kink-antikink collisions (2022).
- Campos J, Mohammadi A, Queiruga J, Wereszczynski A. Fermionic spectral walls in in kink collisions (2023).
- Farhi E, Graham N, Jaffe RL, Weigel H. A heavy fermion can create a soliton: a 1+1 dimensional example. *Phys Lett* (2000) 475B:335–41. doi:10.1016/s0370-2693(00)00108-8
- Sugiyama T. Kink-antikink collisions in the two-dimensional ϕ^4 model. *Prog Theor Phys* (1971) 61:15501563. doi:10.1143/ptp.61.1550
- Campbell DK, Schonfels JS, Wingate CA. Resonance structure in kink-antikink interactions ϕ^4 theory. *Physica* (1983) D9:1–32.
- Alonso-Izquierdo A, Gonzalez Leon MA, Mateos Guilarte J. The Kink variety in systems of two coupled scalar fields in two space-time dimensions. *Phys Rev* (2002) D65:085012.
- Alonso-Izquierdo A, Gonzalez Leon MA, Mateos Guilarte J. Kinks in a non-linear massive sigma model. *Phys Rev Lett* (2008) 101:131602. doi:10.1103/PhysRevLett.101.131602
- Alonso-Izquierdo A, Garcia Fuertes W, Mateos Guilarte J. A note in BPS vortex bound states. *Phys Lett* (2016) B753:29–32.
- Alonso-Izquierdo A, Garcia Fuertes W, Mateos Guilarte J. Dissecting zero modes and bound states on BPS vortices in Ginzburg-Landau superconductors (2016).
- Alonso-Izquierdo A, Garcia Fuertes W, Manton NS, Mateos Guilarte J. Spectral flow of vortex shape modes over the BPS 2-vortex moduli space. *J High Energ Phys.* (2024) 2024:20. doi:10.1007/jhep01(2024)020
- Alonso-Izquierdo A, Manton NS, Mateos Guilarte J, Wereszczynski A. Collective coordinate models for 2-vortex shape mode dynamics. *Phys Rev* (2024) D110:085006. doi:10.1103/physrevd.110.085006
- Alonso-Izquierdo A, Manton NS, Mateos Guilarte J, Rees M, Wereszczynski A. Dynamics of excited BPS 3-vortices. *Phys Rev* (2025) D111:105021.